

Steady light transport under flow: Characterization of evolving dense random media

C. Baravian,* F. Caton, J. Dillet, and J. Mougel

Laboratoire d'Energétique et de Mécanique Théorique et Appliquée, CNRS UMR 7563, 2 Avenue de la Forêt de Haye,
B.P. 160, 54504 Vandoeuvre Cedex, France

(Received 6 May 2004; revised manuscript received 11 March 2005; published 10 June 2005)

We describe in this letter a new rheo-optical apparatus able to measure the photon transport length l^* in an evolving random medium. First, the appropriate solution of the diffusion equation for oil in water, stable, micron-sized emulsions is compared successfully with the measured spatial distribution of incoherent back-scattered light given by the new apparatus. Further validation is provided using stable samples of varying sizes and volume fractions (1% to 64%) and comparing measurements with Mie-Percus-Yevick calculations based on independent small-angle light scattering (SALS) measurements. As a typical example application of the system, the emulsification of a different oil in water system is studied *in situ* and dynamically. The continuous temporal measurements show the decrease of the average size versus time, in excellent quantitative agreement with independent SALS measurements. This evidences that this system is able to probe *continuously* and *nonintrusively* the microscopic and macroscopic flow-induced organization of suspensions.

DOI: 10.1103/PhysRevE.71.066603

PACS number(s): 42.25.Fx, 83.85.Ei, 46.65.+g, 42.30.-d

I. INTRODUCTION

The past two decades have seen the development of non-invasive optical techniques for the quantitative study of random media, ranging from optical tomography (e.g., Refs. [1–4]) to small-angle light scattering (SALS) and diffusive wave spectroscopy (DWS) (e.g., Ref. [5]). This paper is concerned with the presentation of a new tool that allows measurements of the light transport length (l^*) in a dense, evolving system under varying external conditions. For example, the temporal evolution of the microscopic structure of an oil in water emulsion can be monitored while shearing the solution, evolution that is currently inaccessible to the above techniques.

At the time of writing this paper, there are three quite different types of systems that use light as a probe of the mesoscopic structure of materials. The first category is essentially based on SALS, from which, in the very dilute case, information about the size of the suspended objects can be extracted. The second category consists of dynamic light scattering (DLS) and its multiple scattering extensions, e.g., DWS, that measure the diffusion coefficient of the suspended particles. Those techniques have some limitations that impair their use in experiments on evolving dense media. First, they are generally difficult to use in systems with a large unknown macroscopic velocity since the speckles have to be averaged over long enough times at a given position. Also, the use of DLS is limited to low enough concentrations so that the pair interactions are negligible. Finally, in the case of DWS, the system under investigation must be ergodic. This condition is very often not met in concentrated colloidal systems as they exhibit solidlike behaviors [6–8]. The third category of systems evaluates the optical thickness of the medium (i.e., the inverse of the mean free path), mainly by reflectance or transmittance measurements (e.g., Ref. [6]). Those measure-

ments are not easy to perform, first because of the need for a specific calibration using a reference sample in the appropriate range. More importantly, this method cannot separate scattering and absorption, which forbids its use in systems that are even slightly absorbing.

We propose a system that is designed for the simultaneous microscopic and macroscopic characterization of evolving- and optically dense media such as perturbed concentrated suspensions, a system that must be as general and flexible as possible. The basic idea of the optical part of this technique is to use a steady collimated light source and to deduce from the spatial distribution of the incoherent backscattered light the microscopic properties of the random media while varying the external conditions (in our example: shear). The optical part of the method has been through quite extensive theoretical developments and could be coined as “steady light transport.” (SLT) To our knowledge, there are no experiments showing the validity domain of the method, nor its experimental potential to study evolving concentrated media. The aim of our paper is to fill this gap.

We first describe the experimental setup and methods as well as the test materials used for validation purposes. Existing theoretical results are then briefly summarized. Finally, the experimental system is validated and applied to flow-induced emulsification.

II. EXPERIMENTAL SETUP

The experimental setup is sketched in Fig. 1 and contains three main parts. The first part consists of a laser ($\lambda = 632.8$ nm), an optical fiber with its collimator, and a system of mirrors. It produces, guides the laser light, and collimates, it into the sample. The output intensity is stable within 3% (manufacturer datasheets), and is circularly polarized. The second part consists of one circular glass plate of thickness 2 cm, optically treated to avoid reflections. This plate is placed on an AR2000 TA Instrument rheometer. This rheometer controls the vane geometry rotation rate as well as the

*Electronic address: christophe.baravian@ensem.inpl-nancy.fr

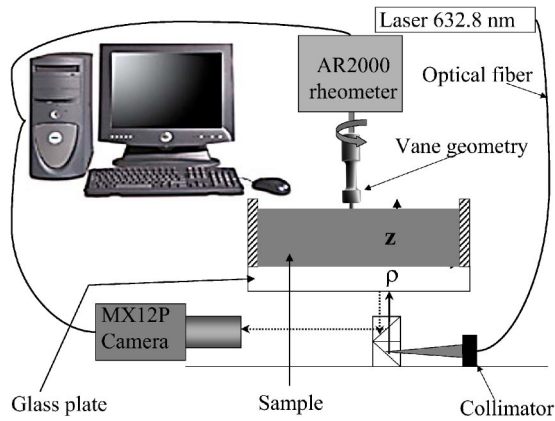


FIG. 1. Sketch of the experimental system.

distance between the plate and the vane (see Fig. 1). This can be used to make the SLT measurements during emulsification experiments, with complete control of the flow parameters. The vane geometry is chosen in order to avoid slip effects in the emulsification of the oil in water solution (see, e.g., Ref. [9]). The third part of the system consists of a digital image acquisition system. An Adimec MX12P digital camera (1024² pixels, 12 bits, 30 frames/s) is linked to an Imasys digital image acquisition card, with a 100 Mo/s transfer rate, controlled by the PC computer. This image acquisition system is also synchronized with the rheometer acquisition system. The acquired image size of the backscattered light is approximately 5 mm, very large compared to the impinging laser spot (50 μ m). The experiments were performed in a climatized room at 20 °C. Thus, the camera noise was held constant within one gray level.

For experiments at rest, ten images are acquired and averaged in order to decrease the speckle and numerical noise. This was less necessary for sheared experiments since the speckles disappear. The gray levels barycenter of the image is then detected and an angular average taken with this barycenter as origin of the polar coordinates. This yields the radial (ρ) distribution of the angular averaged intensity. Equation (3) is then fitted on this radial distribution, giving a measurement of l^* for each sample [see Fig. 2(a)]. All these operations are performed using a home-built C++ program. The adjustments of theoretical curves were performed using standard least-square fit methods.

The validation of the system described in this paper was performed on three different industrial oil-water emulsions, prepared “Firmenich S.A” with three different emulsifiers. The three emulsions, noted STT063, STT046, and STT025, had respective mass fractions of (0.02,0.60,0.38), (0.03,0.60,0.37), and (0.04,0.50,0.46) in (emulsifier, Neobee oil®, and water) and used as emulsifier, respectively, citrem, solutol 80 K, and rice lecithin. The oil refractive index is 1.4564. The size distribution of all three emulsions is plotted in Fig. 2(b) and was determined by SALS using a Malvern Mastersizer S. The angular intensity distribution was inverted to give a size distribution using Malvern’s proprietary software.

III. THEORETICAL BACKGROUND

The theoretical study of the propagation of light in dense (turbid) media has recently been through much development

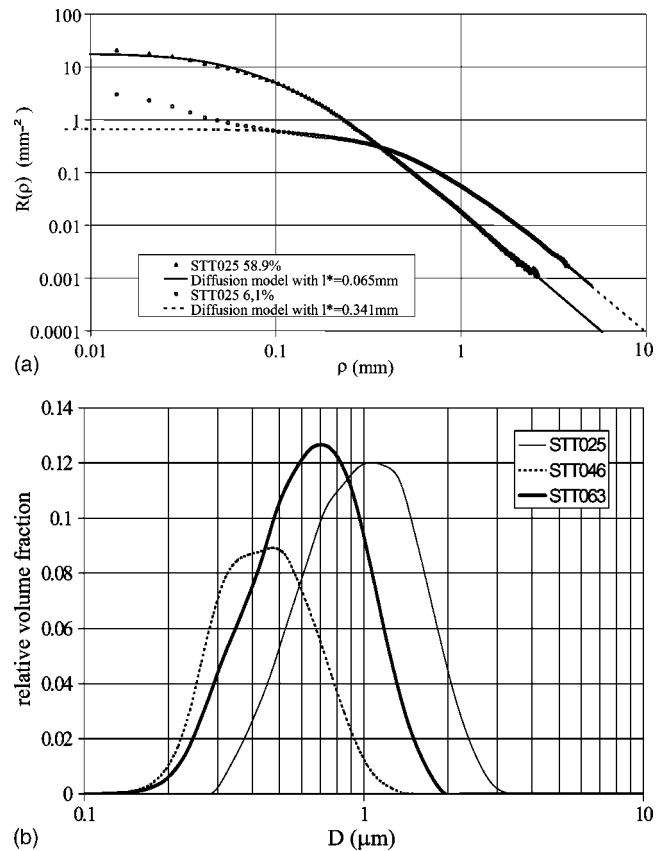


FIG. 2. (a) Two examples fit of experimental curves with Eq. (3). (b) Diameter distributions for the three emulsions.

thanks to its application to optical tomography [2] and possible application to laser light amplification [10]. It is usually modeled—when neglecting coherence and polarization effects—by the radiative transfer equation for the radiance (also called specific intensity) (see Refs. [11,12]). Assuming that the anisotropic part of the radiance is much smaller than the isotropic part, this radiative transfer equation can be reduced to a diffusion equation for the fluence rate with Robin boundary condition, where the fluence is the integral over all solid angles of the radiance (Ref. [11], Chap.7). Haskell *et al.* [12] showed that the rigorous solution to the semi-infinite medium problem with a collimated source can be well approximated using the so-called extrapolated boundary condition and the method of images. The solution is written in cylindrical coordinates, with the origin of coordinates chosen as the point where the beam enters the medium; ρ is the radial coordinate and z the height (See Fig. 1). Neglecting the absorption for simplicity, the steady-state fluence is [13]

$$\Phi(\rho, z) = \frac{3}{4\pi l^*} \left(\frac{1}{((z - l^*)^2 + \rho^2)^{1/2}} - \frac{1}{((z + l^* + z_b)^2 + \rho^2)^{1/2}} \right), \quad \text{with } z_b = \frac{2}{3} l^* \frac{1 + R_{\text{eff}}}{1 - R_{\text{eff}}}. \quad (1)$$

R_{eff} is the fraction of photons internally reflected at the boundary (calculated according to Ref. [12]). l^* is the “trans-

port length” and is the only parameter necessary to describe the diffuse light transport in the medium (see the next paragraph). The measured backscattered signal corresponds to the reflectance

$$R(\rho) = \int_{2\pi} \frac{1 - R_{\text{Fresnel}}(\theta)}{4\pi} \left[\Phi(\rho, z=0) + l^* \frac{\partial \Phi(\rho, z=0)}{\partial z} \cos(\theta) \right] \cos(\theta) d\Omega, \quad (2)$$

where $R_{\text{Fresnel}}(\theta)$ is the usual unpolarized Fresnel reflection coefficient. In our case, since we use a 2 cm thick glass plate that has been treated to avoid reflections at the laser wavelength, and the suspending medium is always water, we will consider that there is no index mismatch. The solution for our experimental system then is

$$R(\rho) = \frac{1}{(l^*)^2} \left[\frac{0.0398}{\left(1 + \left(\frac{\rho}{l^*}\right)^2\right)^{3/2}} - \frac{0.0928}{\left(5.444 + \left(\frac{\rho}{l^*}\right)^2\right)^{3/2}} + 0.0597 \left(\frac{1}{\left(1 + \left(\frac{\rho}{l^*}\right)^2\right)^{1/2}} - \frac{1}{\left(5.444 + \left(\frac{\rho}{l^*}\right)^2\right)^{1/2}} \right) \right]. \quad (3)$$

This theoretical expression is fitted to the experimental data to obtain a measurement of l^* . Besides, $R(\rho)(l^*)^2$ is a nondimensional quantity that yields a universal curve when the radial coordinate ρ is scaled with l^* . This scaling provides a strong test for the validity of the model. Note also that absorption can be easily included in the model and is then simply an additional fit parameter [13], allowing easy discrimination of scattering and absorption.

We present in the following the validation of the measurement method using the stable nonabsorbing micron-sized emulsions described in detail previously. The technique is then used to characterize the emulsification of an oil in water solution under shear.

IV. VALIDATION

As we wish to validate the measurement method of l^* proposed above, we need to compare it with another accepted evaluation of this length. The simplest experimental way is to measure by SALS the size distribution of the emulsions (using a Malvern Mastersizer S) and their concentration (by dry extract) and, knowing from the manufacturer the refractive indexes of the phases, to calculate l^* from those data.

A. Evaluation of l^* using SALS data: Mie-Percus-Yevick calculations

In dilute monodisperse systems, the transport length l^* can be calculated using Mie theory, and is defined as $l^* = 1/[nC_{\text{scat}}(1-g)]$, with C_{scat} the scattering cross section, g the scattering anisotropy parameter, and n the number density of particles (see, e.g., Ref. [14]). We need to calculate

this length for *polydisperse and concentrated* emulsions, in which case it is not clear if an analytical calculation of $\langle C_{\text{scat}} \rangle$ and $\langle g \rangle$ is possible, even if the pair structure factors for the different particle classes can be calculated. So, we resort to the following two-step approximation. First, neglecting the effect of high concentrations, we determine an equivalent monodisperse medium accounting for the polydispersity. Second, we apply the Percus-Yevick correction [15] to this monodisperse equivalent medium.

The first step starts by calculating the effect of polydispersity on the transport length. For a histogram of N class of particles sizes, the average scattering parameters are [16]

$$\langle \mu_{\text{scat}} \rangle \equiv \langle n(i) C_{\text{scat}}(i) \rangle = \sum_{i=1}^N \mu_{\text{scat}}(i); \quad (4)$$

$$\langle g \rangle = 2\pi \int_0^\pi \frac{\sum_{i=1}^N P(\theta, i) \mu_{\text{scat}}(i)}{\langle \mu_{\text{scat}} \rangle} \cos(\theta) \sin(\theta) d\theta,$$

where $C_{\text{scat}}(i)$, $n(i)$, and $P(\theta, i)$ are, respectively, the scattering cross section, the number density, and the phase function for particles of size within the class i . The transport length is then $\langle l^* \rangle = 1/[\langle \mu_{\text{scat}} \rangle (1 - \langle g \rangle)]$, this expression accounting for the polydispersity of the sample. The equivalent monodisperse medium is determined in the diluted regime by finding its equivalent size $\langle a \rangle$ for which $l^*(\langle a \rangle) = \langle l^* \rangle$, for constant total volume fraction, optical indexes, and wavelength.

The second step of the calculus applies the standard Percus-Yevick correction [6] to this monodisperse equivalent medium to evaluate $C_{\text{scat}}^{\text{PY}}(\langle a \rangle)$ and $g^{\text{PY}}(\langle a \rangle)$, from which we deduce $l^{*\text{PY}}(\langle a \rangle)$. In the following paragraph concerning the validation of the measurement method, experimental SLT measurements of l^* are compared to this value.

B. Mean size variations

In all experiments, a constant medium thickness of 40 mm was used. This thickness is large enough compared to the measured l^* to ensure that the semi-infinite medium approximation is valid.

We show that the steady light transport technique determines l^* in a very robust manner, first by varying the mean size of the suspended particles. Steady light transport experiments were performed with the STT063, STT046, and STT025 emulsions at a respective volume fraction of 63.8%, 64.7%, and 58.9%.

Equation (3) is fitted on each experimental curve using a least-square fit, giving a measurement of l^* [see, e.g., Fig. 2(a)]. Each experimental curve is then rescaled by $(l^*)^2$ and plotted against ρ/l^* , as suggested by the scaling of Eq. (3). The three curves obtained for the three different sizes are shown in Fig. 3 along with the theoretical curve [Eq. (3)]. The experimental curves and the diffusion model agree perfectly over more than 3 decades of intensity, collapsing nicely on a single curve from $\rho/l^* \approx 1$ to ∞ . This excellent rescaling validates the diffusion model.

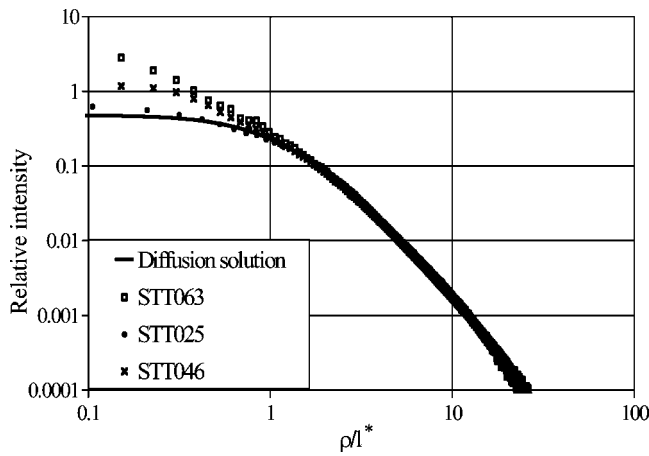


FIG. 3. Scaled experimental data and diffusion model.

C. Successive dilutions

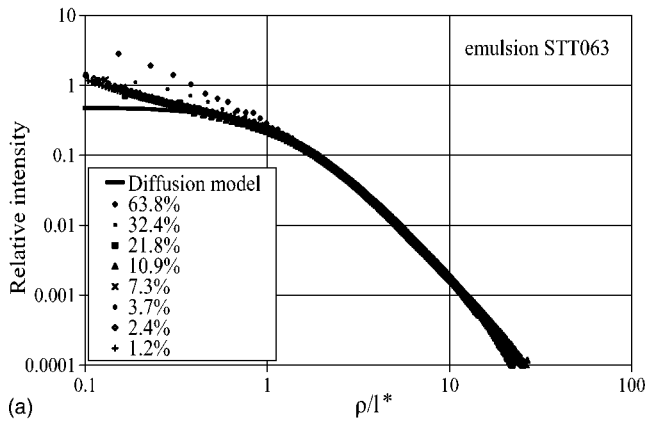
In order to assess the robustness of the measurement method, we also conducted a series of light transport experiments for successive dilutions, yielding volume fractions ranging from a few percent to the random packing volume fraction. As in the previous paragraph, the curves collapse very well when rescaled by $(l^*)^2$ and plotted against ρ/l^* [see

Fig. 4(a)], further confirming the robustness of the method.

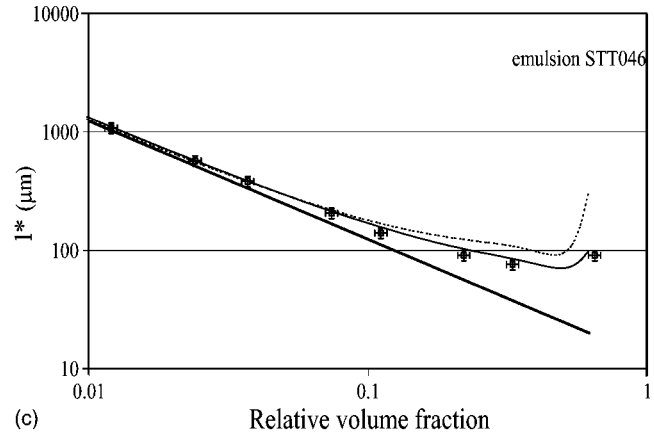
D. Comparison with SALS measurements

Finally, we compare the variation of l^* measured above and the theoretical values computed by the polydisperse Percus-Yevick approximation using the size distributions measured by SALS [Fig. 2(b)]. In all three figures [Figs. 4(b)–4(d)] the thick straight line corresponds to polydisperse dilute Mie calculations, the dashed curve corresponds to the polydisperse Mie-Percus-Yevick approximation. The continuous curve corresponds to the same calculation with an increase of 1% of the refractive index of the oil given by the manufacturer.

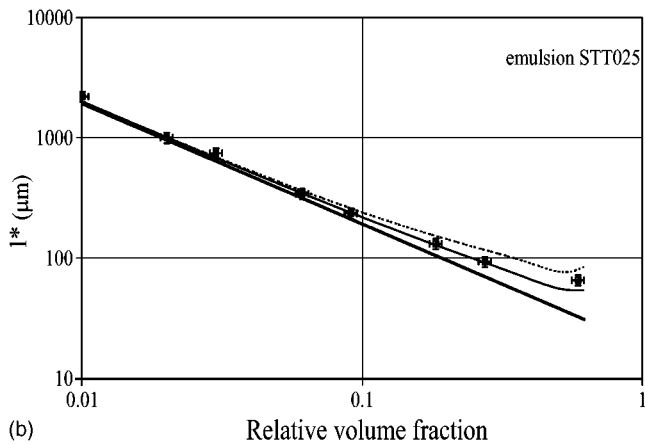
The general agreement is very good, being excellent for concentrations smaller than 10%. An *a priori* surprising result is the large sensitivity of the method to small differences in refractive indexes. Recalling that we use a *backscattering* geometry, we are sampling the *whole* phase function, including large angles. This part of the phase function is more sensitive to small differences in the refractive index than the small angles part used in the standard SALS techniques. Since the emulsifier added to the oil to stabilize the solution are polar molecules, it is to be expected that the refractive index of the oil-polymer solution will be an increasing func-



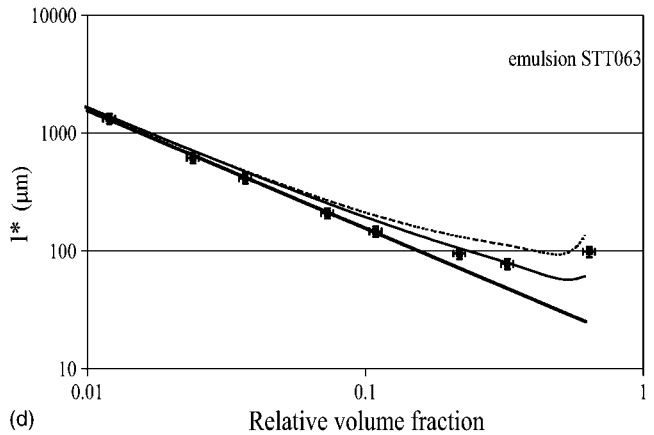
(a)



(c)



(b)



(d)

FIG. 4. (a) Rescaling of experimental data from successive dilution experiments and of the diffusion solution. (b) STT025 SLT measurements versus Mie and PY calculations. (c) STT046 SLT measurements versus Mie and PY calculations. (d) STT063 SLT measurements versus Mie and PY calculations.

tion of the relative concentration in polymer, which explains the necessity to adjust slightly the refractive index.

The validation presented here is an extensive comparison between the measured spatial distribution of backscattered light and the theoretical curves when varying two of the three parameters controlling light scattering. Indeed, both the size and the volume fraction were varied, the latter in a considerable range (1.2% to 63.8%). The consequence of this large variation is an even larger variation in l^* over nearly 2 decades. Also, we should underline that no specific calibration of the apparatus is needed, unlike optical thickness measurements. Moreover, as is clear from diffusion theory [13], this method can discriminate between absorption and diffusion, information that cannot be obtained from optical thickness measurements. Finally, it is noteworthy that the industrial samples we used were not tailored for validation purposes, showing the excellent flexibility and versatility of the method.

V. APPLICATION: SHEAR INDUCED EMULSIFICATION

We now apply the new technique to study flow-induced oil in water emulsification. Steady light transport measurements were performed at regular time intervals (30 min) during the first day after the start of the experiment, the experiment lasting approximately 2 days. After simply filling the system with 50% hexadecane oil and 48% water premixed with 2% modified dextrane, a constant rotation rate of 100 rad/s was applied to the vane geometry. This experiment was performed twice, yielding identical results. The emulsion was sampled at one time during the experiment and also at the end to perform Malvern measurements in order to compare the SLT measurements to polydisperse Mie-Percus-Yevick calculations [Fig. 5(a)]. First, we observe an excellent agreement between the SLT measurements and polydisperse Mie-Percus-Yevick calculations, further validating our apparatus and methods. In Fig. 5(a) a clear decrease of l^* versus time is observed, a decrease that converges to a constant value. From those data, since the experiments are performed at constant volume fraction and constant refractive indexes, the Mie-Percus-Yevick problem can be inverted to obtain the evolution of the equivalent average size, which is plotted in Fig. 5(b). This shows that this apparatus may be used to study or monitor quantitatively the emulsification process in a continuous and nonintrusive way.

VI. CONCLUSION

In conclusion, we have shown in this paper that our experimental apparatus and methods are able to measure *under flow*, and in a dense and opaque random media, the photon transport length l^* . Indeed, after extensively validating the measurement method and the theoretical analysis against

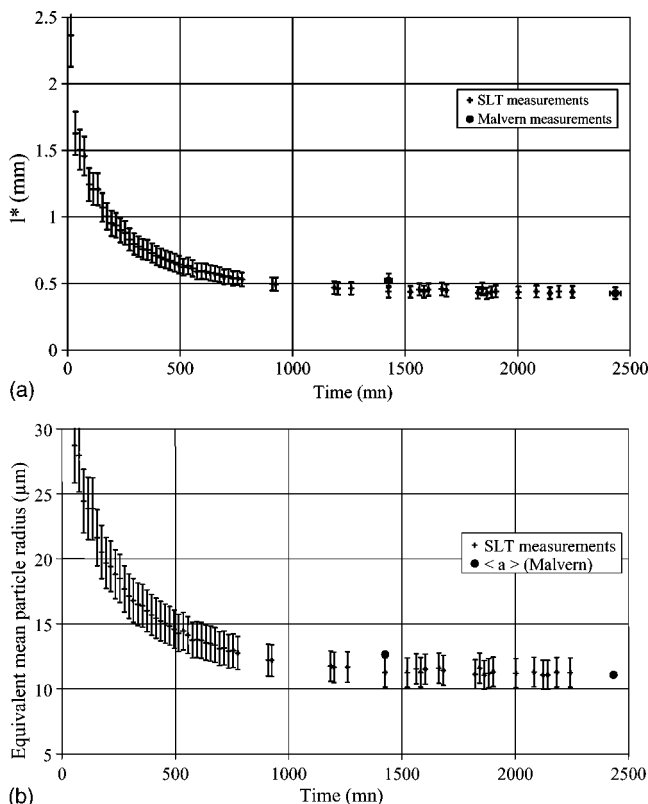


FIG. 5. Shear induced emulsification of the hexadecane and water emulsion. (a) Transport length l^* versus time. (b) Equivalent average droplet size versus time.

standard SALS measurements, we have demonstrated that this tool allows continuous *in situ* monitoring of an emulsification process, and in particular allows one to measure the temporal evolution of an average droplet size.

We believe that this tool is of considerable interest since it is much more versatile than optical depth measurements as it is not limited by evolving concentration, size, or optical properties. As it still uses light as a probe, this tool should indeed be very useful to analyze the relationship between the microscopic to macroscopic organization of fast-evolving condensed matter, applicable to suspensions, powders, or foams. Conversely, this system could also be implemented for online quality monitoring in industrial production batches or flows.

ACKNOWLEDGMENTS

We thank S. Tupin, F. Vigouroux, and A. Parker from Firmenich S.A. for preparing the samples and providing part of the financial support for J. Dillet. We are grateful to Dr. A. Durand for supplying modified dextran.

- [1] A. Polishchuk, T. Dolne, F. Liu, and R. Alfano, *J. Opt. Soc. Am. A* **22**, 430 (1997).
- [2] S. Arridge, *Inverse Probl.* **15**, R41 (1999).
- [3] J. Paasschens, Ph.D. thesis, Leiden University, Netherlands (1997).
- [4] S. Prael, Ph.D. thesis, University of Texas (1988).
- [5] D. Pine, D. Weitz, P. Chaikin, and E. Herbolzheimer, *Phys. Rev. Lett.* **60**, 1134 (1989).
- [6] L. Rojas-Ochoa, S. Romer, F. Scheffold, and P. Schurtenberger, *Phys. Rev. E* **65**, 051403 (2002).
- [7] J. Z. Xue, D. J. Pine, S. T. Milner, X. L. Wu, and P. M. Chaikin, *Phys. Rev. A* **46**, 6550 (1992).
- [8] F. Scheffold, S. Skipetrov, S. Romer, and P. Schurtenberger, *Phys. Rev. E* **63**, 061404 (2001).
- [9] C. Baravian, A. Lalante, and A. Parker, *Appl. Rheol.* **12**, 81 (2002).
- [10] K. Yoo, K. Arya, G. Tang, J. Birman, and R. Alfano, *Nonlinear Opt.* **3**, 149 (1992).
- [11] A. Ishimaru, *Wave Propagation and Scattering in Random Media* (IEEE Press, Piscataway, NJ/Oxford University Press, Oxford, 1997).
- [12] R. Haskell, L. Svaasand, T. Tsay, T. Feng, and S. McAdams, *J. Opt. Soc. Am. A* **11**, 2727 (1994).
- [13] A. Kienle and M. Patterson, *J. Opt. Soc. Am. A* **14**, 246 (1997).
- [14] C. Bohren and D. Huffman, *Absorption and Scattering of Light by Small Particles* (Wiley, New York, 1983).
- [15] L. Tsang, J. Kong, K. Ding, and C. Ao, *Scattering of Electromagnetic Waves, Volume II: Numerical Simulations* (Wiley, New York, 2001).
- [16] J. R. Mourant, J. Freyer, A. Hielscher, A. Eick, D. Shen, and T. Johnson, *Appl. Opt.* **37**, 3586 (1998).